J Solid State Electrochem (2011) 15:2601–2610
DOI 10.1007/s10008-010-1253-z

ORIGINAL PAPER

The study on microstructure and electrochemical properties of Al–Mg–Sn–Ga–Pb alloy anode material for Al/AgO battery

Zhengqing Ma · Xiaoxiang Li

Received: 21 August 2010 / Revised: 10 November 2010 / Accepted: 15 November 2010 / Published online: 1 December 2010

Abstract The microstructure of Al–Mg–Sn–Ga–Pb quinary aluminum alloy anode material and the influences of its electrochemical properties and self-corrosion rate in 4 mol/l NaOH +10 g/l Na_2SnO_3 medium were studied. The microstructure and morphology were characterized by metallographic microscope, transmission electron microscope, and scanning electron microscopy. The electrochemical properties were tested by electrochemical workstation, and the self-corrosion rate of Al alloy anode was studied by methods of recovery H_2 gas by discharge water. The results show that homogenization has not much impact on the electrochemical properties and the corrosion rate of the cast aluminum alloy anode material; besides, return annealing treatment of the cold-rolled Al–Mg–Sn–Ga–Pb quinary aluminum alloy anode material can reduce the rate of self-corrosion and make Al anodic potential shift negative steadily and improve the properties of the material.

Keywords Al alloy anode · Heat treatment · Microstructure · Electric potential · Corrosion

Introduction

Aluminum is an attractive choice for galvanic anode in primary alkaline batteries due to its attractive properties such as high specific energy and high current density in alkaline medium as well as its abundance, low cost, and light mass [1–4]. And the specific energy of Al/AgO battery containing aluminum as anode is 1,090 Wh/kg, which is close to twice of that of Mg/AgCl (450 Wh/kg) and Zn/AgO (540 Wh/kg). Al anode battery can be applied in the power source of unmanned underwater vehicle propulsion system, such as the utilization of emergency power sources and fieldwork electrical sources. Al anode may be developed to the power sources of electrical automobile due to its merit of pollution free [5–8]. And Al–Mg–Sn–Ga–Pb quinary aluminum alloy anode is a kind of material for Al/AgO battery.

As the compatibility, density, and melting point are different between the alloying elements and the substrate aluminum, the metal ingot casting organizations are uneven during solidification and cause some casting defects, such as non-uniform composition, shrinkage, loose, and bubbles [9, 10]. Therefore, the metal ingot should be under homogenization treatment and then followed with pressing to reduce the casting defects [11].

Under the interaction of tensile stress and compressive stress, the metal ingot will have plastic deformation. On the one hand, crystal particles are elongated to pinstriped shape or the fiber shape which is called “fiber organization” [12]. Meanwhile, the crystal boundary becomes fuzzy. On the other hand, with the occurrence of deformation, the dislocations become entangled; the grains break into smaller sub-grains, the substructure inside also has significant changes, and all these lead variation of electrochemical properties [13–18].

The main purpose of the current work is to investigate the influences of homogenization and annealing treatment after plastic deformation on the microstructure, the corrosion rate, and the electrochemical properties of aluminum alloy anode material.

Z. Ma · X. Li (✉)
School of Materials Science and Engineering,
Central South University,
Changsha 410083, China
e-mail: l-xiaoxiang@163.com

Experimental

Al–Mg–Sn–Ga–Pb aluminum alloy anode material (serial number is AM0501 and the percentages of the alloying elements are Al–0.5Mg–0.1Sn–0.02Ga–0.1Pb) was prepared by adding the alloying elements into the high pure Al solution. After the process of smelting, degassing, standing, and slag off in 750 °C in resistance furnace, the melt was cast into 250×200×22-mm water-cooled model and become the aluminum alloy ingots.

Heat treatment The homogenization treatment was carried out in the box-type electric resistance furnace.

Whole process The whole process was milling surface, hot-rolled to 8.0 mm at 420 °C, intermediate stress relief annealing at 400 °C for 2 h, cold-rolled into 0.45-mm-thick sheet, cold deformation is 94.4%, and then annealing.

Metallurgical specimens were cut and prepared from as-cast ingots, homogenized ingots, and heat-treated sheets. The microstructures were investigated by Polyvar-MET metallographic microscope and Tecnai G220 transmission electron microscope (TEM). Electrolytic polishing liquid for the alloy and its technological conditions were as follows: the mixture of 20% perchloric acids (10 ml) and anhydrous ethyl alcohol (90 ml), polishing voltage 18 V, polish time 15 s, and electrolyte temperature <40 °C.

Anode coating fluid is 95–98%, sulfuric acid is 38%, 85% phosphoric acid is 43%, and distilled water is 19 ml. The process parameters of anodic coating are as follows: voltage 20 V, time 3 min, and temperature <40 °C.

Surface topography The superficial appearance was observed with a Sirion 200 field launch scanning electron microscope and Genesis 60 s was used to analyze the corrosion products on the surface of anode.

DTA Differential thermal analysis was carried out by Rigaku Corporation thermal analyzer. The initial temperature was 400 °C, and the termination temperature was 700 °C with a heating rate of 10 °C/min.

Electrochemical properties The electrochemical properties were tested by electrochemical workstation. The working electrode is Al alloy, the sample's surface area is 1 cm^2, and volume of the corrosion solution is 200 ml. The counterelectrode is Pt and the surface area is 4 cm^2. The medium of working electrode and counterelectrode is 4 mol/l NaOH +10 g/l Na_2SnO_3 (Na_2SnO_3 is used for slow release formulation). The reference electrode is Hg/HgO, and the medium is 1 mol/l NaOH.

The self-corrosion rate of Al alloy anode It is studied by methods of recovery H_2 gas by discharge water. H_2 is gathered by alkali burette. The accuracy of the alkali burette is 0.1 ml.

Results and discussion

Effects of homogenization treatment on the microstructure and properties of AM0501 Al alloy anode material

The process parameters of homogenization on AM0501 Al alloy anode material is shown in Table 1.

Microscopic constitutions

The metallurgical micrographs of AM0501 aluminum alloy ingot after different homogenization treatment processes are shown in Fig. 1. From Fig. 1a, we know that AM0501-cast aluminum alloy anode ingot has uniform α-Al equiaxed grains. AM0501 has clear grain boundary and small amount of casting defects, such as dislocation. After isothermal treatment at 450 °C for 6 h, the grain size is similar to that of non-treated ingots, but the grain boundary becomes clearer [19] (see Fig. 1b). After isothermal treatment at 550 °C for 6 h, grain size grows slightly. Fine dispersed precipitates appear inside the crystal and around the grain boundary. Meanwhile, casting defects reduce (see Fig. 1c). After isothermal treatment at 600 °C for 6 h, the grains grow obviously and its grain size is much larger than that of not treated ingots. There are some small, uneven precipitates at the grain boundaries, as shown in Fig. 1d.

Hydrogen evolution rate

After different homogenization treatments, the hydrogen evolution rate of AM0501-cast aluminum alloy anode material in 4 mol/l NaOH+10 g/l Na_2SnO_3 medium is shown in Fig. 2. From Fig. 2a, the hydrogen evolution rate of cast aluminum alloy anode almost does not change with the extension of the homogenization time (at the same

Table 1 Parameters of homogenizing treatment (cooling medium: tap water 25 °C)

Temperature (°C)	Time (h)		
25	–	–	–
450	2	6	12
500	2	6	12
550	2	6	12
600	2	6	12

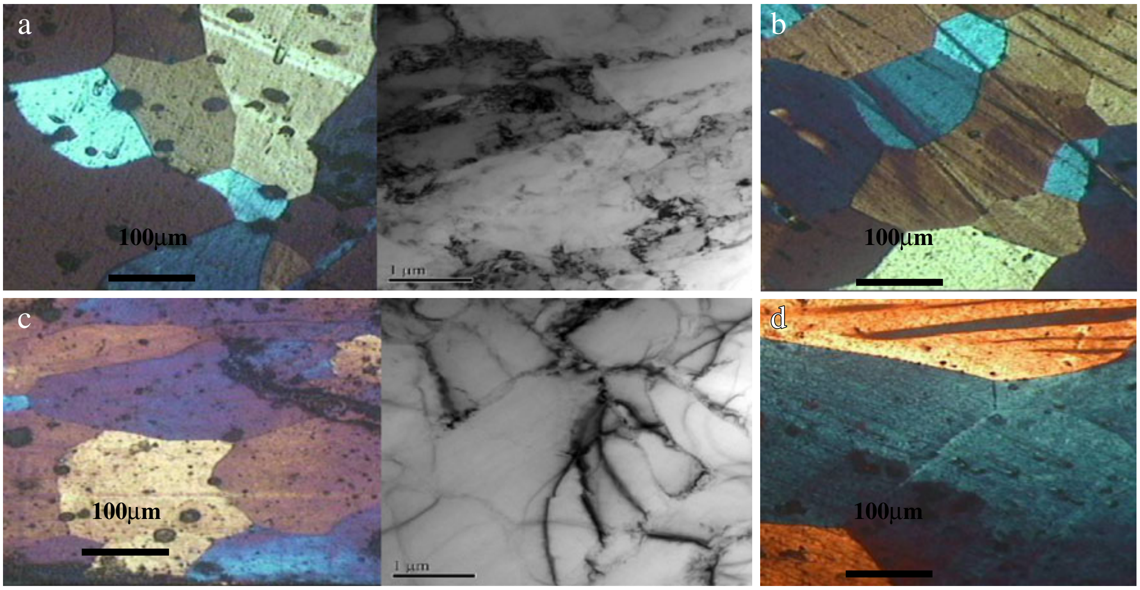

Fig. 1 Metallurgical micrographs of AM0501 Al alloy anode sheet after different annealing treatment. **a** cast–×50, ×40,000; **b** 450 °C–6 h–×50; **c** 550 °C–6 h–×50, ×40,000; **d** 600 °C–6 h–×50

annealing temperature). With the change of temperature, the three kinds of treated cast aluminum alloy (500 °C—3, 6, and 12 h; 550 °C—3, 6, and 12 h; and 600 °C—3, 6, and 12 h) all have small hydrogen evolution rate at 25 °C, and the rates are 0.047, 0.045, and 0.048 ml cm^{-2} min^{-1}, respectively. Among them, the rate of which keeping at 550 °C for 6 h is the minimum. The hydrogen evolution rate increases a few with the increase of homogenization temperature at 80 °C. After keeping at 500 °C, 550 °C, and 600 °C for 2 h, hydrogen evolution rates are 0.22, 0.22, and 0.24 ml cm^{-2} min^{-1}, respectively. After keeping at 500 °C, 550 °C, and 600 °C for 12 h, hydrogen evolution rates are 0.26, 0.28, and 0.32 ml cm^{-2} min^{-1}, respectively. It is suggested that homogenization annealing process of the AM0501-cast aluminum alloy anode has few effects on hydrogen evolution rate in 4 mol/l NaOH+10 g/l Na_2SnO_3 medium, and corrosion rates are quite small. The main reason is that homogenization is a combination of dissolution and precipitation. The influences of homogenization on the AM0501 alloy are two sides. On the one hand, thermal stress can be eliminated, the diffusion of alloying elements can be speeded up, alloying elements can be spread evenly and homogeneous solid solution formed, and the number of precipitates at the grain boundary and the grain boundary corrosion and micro-galvanic cell corrosion is reduced [20–25]. Moreover, these cause the corrosion in alkaline media more uniform and the corrosion rate decrease. On the other hand, the alloying elements precipitated and aggrandized with the increase of homogenization temperature and heat preservation time. And these make the hydrogen evolution rate in alkaline medium a slight increase [22, 26].

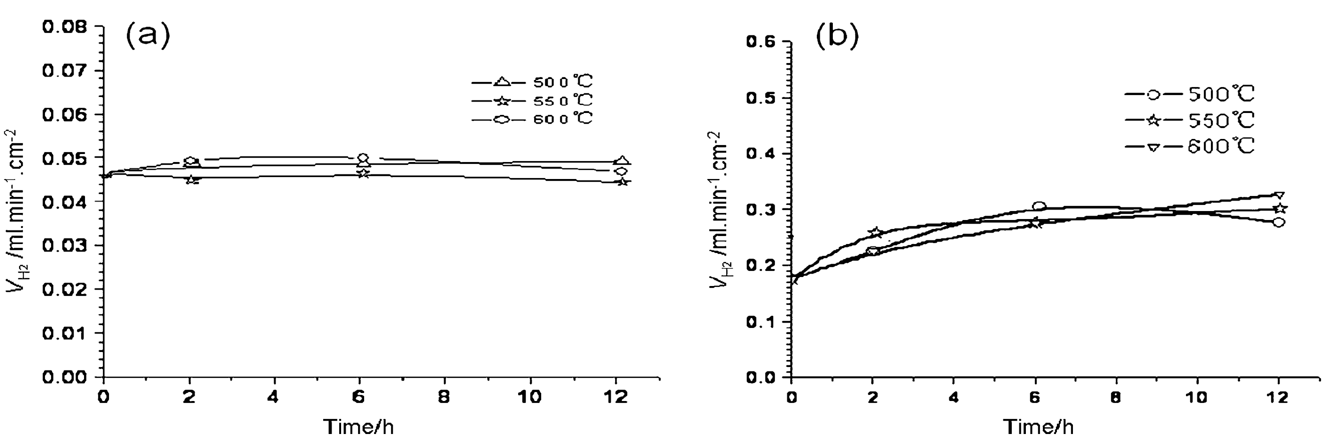

Fig. 2 Hydrogen evolution rate of AM0501 Al alloy anode material after homogenizing treatment. **a** 25 °C 4 mol/l NaOH+10 g/l Na_2SnO_3, **b** 80 °C 4 mol/l NaOH+10 g/l Na_2SnO_3

Electrode potential

The open circuit potential and stable potential of AM0501 Al alloy anode materials via different homogenization treatments are shown in Table 2. From the table, we can see that the open circuit potential of cast AM0501 alloy does not have obvious changes with the increase of homogenization temperature and heat preservation time in 25 °C and 80 °C 4 mol/l NaOH+10 g/l Na_2SnO_3 medium. The voltage is between −1.79 and −1.85 V; therefore, homogenization annealing treatment has few effects on the aluminum anode open circuit potential. Besides, when the anodic polarization ampere density is 200 mA/cm^2, stable potential is between −1.7 and −1.75 V; when the anodic polarization ampere density is 800 mA/cm^2, stable potential is between −1.535 and −1.565 V. With the increase of homogenization temperature and heat preservation time, the stable potential shifts positive a little. After the homogenization treatment at 500 °C, the ingredient is non-uniform, so electronic potential fluctuation is relatively large. After the homogenization treatment at 550 °C, the component is comparatively homogeneous, the discharge potential curve is stable, and electric potential is more negative. After the homogenization treatment at 600 °C, highly active alloying elements solute in the matrix and the depolarization of alloying elements is weak, electric potential shifts positive slightly, but the discharge potential curves is stable. In alkaline medium, the aluminum anode has a high electrochemical activity.

Effects of the final annealing process on the microstructure and properties of AM0501 Al alloy anode material

Microstructure

According to AM0501 alloy composition, the recrystallization temperature can get from pure metal industrial empirical formula: T_{re}=(0.3~0.4) T_m. Thus, recrystallization temperature of AM0501 aluminum alloy anode is about 270~360 °C, and AM0501 alloy melting point is 642.3 °C, which is 915.3 K (shown in Fig. 3). Therefore, the final annealing temperature of aluminum alloy anode plate can be set at 250 °C, 300 °C, and 350 °C, and annealing process is shown in Table 3.

Figure 5 shows the metallographic photos of the rolled AM0501 aluminum alloy anode plate at 250 °C, 300 °C, and 350 °C. From Fig. 5 a, the AM0501 aluminum alloy ingot inner had some changes after the rolling process (cold rolling reduction volume, ~94%), the original equiaxed grains were elongated along the deformation direction into thin strips or fibrous organizations, the fibers along the direction of metal rheological formed a thin strip of “deformed cell”, and a large number of defects such as dislocations and dislocation tangles came out [27–29]. After annealing at 250 °C for 3 h, its microstructure had no significant improvement in the organization and still fibrous, slender strips of “deformed cell” still existed and sub-grains occurred (Fig. 5 b1). The grain boundaries in its initial reply stage were still unclear, residual stress was in relaxation, and large numbers of dislocations still existed. Figure 5 b2 shows the microstructure of aluminum alloy anode via annealing at 250 °C for 6 h. After annealing at 250 °C for 6 h, lath organization in aluminum anode had disappeared to form small angle sub-grain boundaries, the matrix began to form dispersed “primary crystal” in the sub-crystal phase, grain structure formed without noticeable grain boundaries, dislocation density decreased, and the organization redistributed [30]. The precipitate increased obviously, but its distribution was still even and tiny (Fig. 6a). Figure 5 b3 shows the microstructure of aluminum alloy anode via annealing at 250 °C for 10 h. In some parts of aluminum anode matrix, the spaces of sub-grain boundary increased, sub-crystal grew up, part of the shaping grain formed, dislocations almost disappeared, but the grain size was still very small. These showed that this stage was the end of recovery annealing and the initial stage

Table 2 Open circuit potential and stable potential of AM0501 Al alloy anode material (vs. Hg/HgO)

Potential homogenization	Open circuit potential (V)		Stable potential (V)	
	25 °C	80 °C	200 mA/cm^2, 80 °C	800 mA/cm^2, 80 °C
500 °C, 2 h	−1.79	−1.81	−1.702	−1.510
500 °C, 6 h	−1.81	−1.81	−1.721	−1.521
500 °C, 12 h	−1.82	−1.82	−1.722	−1.525
550 °C, 2 h	−1.81	−1.82	−1.721	−1.540
550 °C, 6 h	−1.84	−1.83	−1.741	−1.562
550 °C, 12 h	−1.80	−1.84	−1.746	−1.552
600 °C, 2 h	−1.80	−1.82	−1.705	−1.531
600 °C, 6 h	−1.83	−1.83	−1.721	−1.522
600 °C, 12 h	−1.83	−1.83	−1.722	−1.520

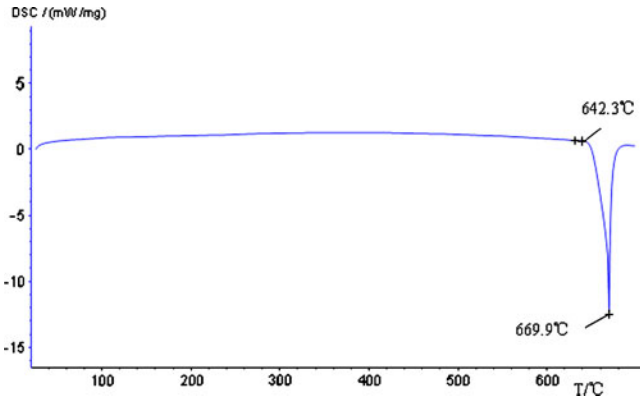

Fig. 3 DSC curve of AM0501 Al alloy

of recrystallization, precipitate increased further, but precipitate was still very evenly distributed (Fig. 4).

Figure 5 C shows the microstructure of AM0501 cold-rolled aluminum alloy anode plates via different annealing holding times at 300 °C. From Fig. 5 C1, we can see that aluminum alloy anode microstructure reply process had been completed and the recrystallization process started after annealing at 300 °C for 3 h, and its microstructures were similar with that of annealing at 250 °C for 10 h. It showed that the cold processed aluminum alloy anode plate was still in the early annealing stage and recrystallization stage after annealing at 300 °C for 3 h, recrystallization grain began to emerge, and part of the new grains replaced the old lath grains. Figure 5 C2 shows that sub-grain boundaries completely disappeared and formed a large number of small multilateral grains after annealing at 300 °C for 6 h. Figure 5 C3 tells that multilateral grain by moving and merging formed a new organization after annealing at 300 °C for 10 h, grain boundary became very clear, recrystallization had been completed, and there were no significant changes in crystal grain size. After annealing at 350 °C for 3 h, the processed structure of aluminum alloy anode plate was completely disappeared into a typical recrystallization organization, but the grain did not grow up (Fig. 5 d1). After annealing at 350 °C for 6 h and at 350 °C for 10 h, fine-grained microorganization was almost disappeared and became coarse equiaxed recrystallization texture, forming a relatively uniform coarse grain, which is shown in Fig. 5 d2, d3. The black part shown in Fig. 6b is obvious precipitates which occur in the grain boundary. The precipitate composition is shown in Fig. 4.

Corrosion morphology

Figure 7 shows the corrosion morphology of AM0501 aluminum alloy anode plate which treated by different annealing processes at 25 °C in 4 mol/l NaOH media. From the figure, we can see that corrosion points were diffusing in the cold-rolled aluminum alloy anode plate, the surface corrosion was uniform, and there was no obvious grain boundary corrosion. Because the low solubility of alloying elements such as Sn, Pb, and other elements precipitated in the grain boundary and formed a cathode phase, heat-treated aluminum anode plate began to appear grain boundary corrosion. At the same time, large quantities of highly active cube texture occurred because cube texture increased and (100) surface had high activity and low corrosion resistance, the corrosion process along the crystallographic orientation, dissolved in a certain rate to keep the aluminum anode in alkaline corrosive [31–33]. The corrosion channel wall along the (100) surface developed and so to form uniform corrosion pits (see Fig. 8c, d). With the increase of cube texture, the erosion depth deepened, the surface area increased, and the grain boundary corrosion was so serious that it led to grain shedding.

Effects of the final heat treatment on properties of AM0501 aluminum alloy anode

Hydrogen evolution rate

After treated by different annealing processes, the static hydrogen evolution rate of cold-rolled AM0501 aluminum alloy plates in 4 mol/l NaOH +10 g/l Na_2SnO_3 medium was shown in Fig. 8. From Fig. 8a, we can see that the rolled aluminum alloy had a larger hydrogen evolution rate in 4 mol/l NaOH +10 g/l Na_2SnO_3 medium due to cold-rolled aluminum alloy sheet that had high stress and high density of dislocations and point defects. The rate at 25 °C medium is about 0.05 ml cm^{-2} min^{-1} and at 80 °C medium is about 0.28 ml cm^{-2} min^{-1}. After annealing at 250 °C for 3 h, some of the internal metal point defect and dislocation led to some changes within the crystal, but the grain size and shape of metal did not have significant changes and the metal still had a high internal stress so the hydrogen evolution rate was large. The rate at 25 °C medium is about 0.045 ml cm^{-2} min^{-1} and at 80 °C medium is about 0.27 ml cm^{-2} min^{-1}. During the annealing treatment at 250 °C for 6 h, 250 °C for 10 h, and 300 °C for 3 h, the

Table 3 Final annealing process of AM0501 aluminum alloy anode plates

Temperature	Time		
	3 h	6 h	10 h
250	250 °C, 3 h	250 °C, 6 h	250 °C, 10 h
300	300 °C, 3 h	300 °C, 6 h	300 °C, 10 h
350	350 °C, 3 h	350 °C, 6 h	350 °C, 10 h

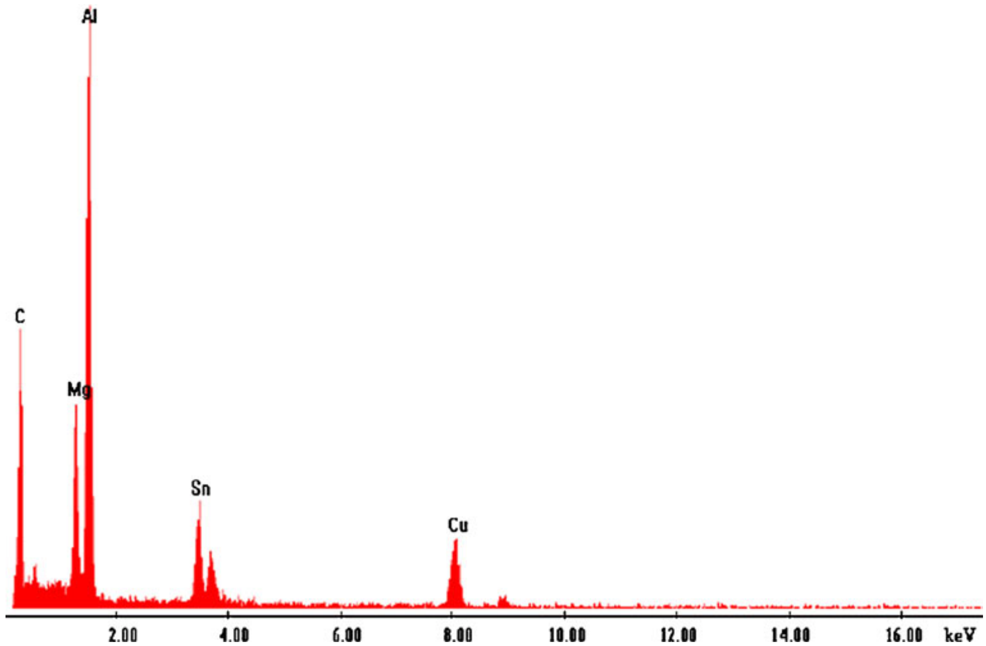

Fig. 4 EDS of AM0501 Al alloy anode sheet

internal stress caused by cold processing decreased, point defects and the energy of lattice distortion also decreased, but the broken crystal stretched state of the whole metal had not changed and the organization was still in re-annealed state. Hydrogen evolution rate decreased, and the rate at 25 °C medium is about 0.04 ml cm^{-2} min^{-1} and at 80 °C medium is about 0.22 ml cm^{-2} min^{-1}. After annealing at 300 °C for 6 h, recrystallization basically completed and formed a fine equiaxed grain, the phenomenon of work hardening basically eliminated, and the stress reduced. There were a few intragranular precipitates (see Fig. 4c). With a large number of cube textures, corrosion accelerated and hydrogen evolution rate had a growing trend. The rate at 25 °C medium is about 0.042 ml cm^{-2} min^{-1} and at 80 °C medium is about 0.23 ml cm^{-2} min^{-1}. After annealing at 300 °C for 10 h and at 350 °C for 3 h, recrystallization had fully completed and a few grains grew, intragranular precipitates and the static hydrogen evolution rate increased, and the rate at 25 °C medium is about 0.046 ml cm^{-2} min^{-1} and at 80 °C medium is about 0.26 ml cm^{-2} min^{-1}. After annealing at 350 °C for 6 h and at 350 °C for 10 h, a large number of intragranular precipitates appeared because of the grain coarsening (see Figs. 4d and 5b). Cube texture increased a lot, reaching 63%. Along the [111] surface, the corrosion depth deepened and the contact area with the lye increased, so the corrosion rate increased further and hydrogen evolution rate also increased. The rates at 25 °C medium are, respectively, 0.048 and 0.052 ml cm^{-2} min^{-1}. The rates at 80 °C medium are, respectively, 0.28 and 0.30 ml cm^{-2} min^{-1}. These showed that the hardening was just completely eliminated after annealing at 250 °C for 6 h and at 250 °C for 10 h, and the cool-rolled aluminum alloy anode plates were at the initial stage of recrystallization, forming a fine grain with no precipitate coarsening or balling, thereby the metal had a small hydrogen evolution rate, that is, a low corrosion rate, which helps to improve the current efficiency of aluminum anode.

Electrode potential

At different annealing temperatures, the galvanostatic discharging curves of AM0501 aluminum alloy anode plate in 4 mol/l NaOH +10 g/l Na_2SnO_3 medium are shown in Fig. 9. From the figure, we can see that the stable potential of unannealed aluminum alloy anode AM0501 is about −1.728 V. Because of the uneven distribution of internal high residual stress and the uneven of point defects, dislocations, and other microstructure, its discharge curve was unstable and volatile. During different annealing processes, AM0501 aluminum alloy anode materials had some changes. Stress relieved, energy storage became lower, and the dislocation density decreased. And because cube texture increased, the corrosion depth along the [111] surface deepened and aluminum surface area increased; thus, aluminum surface current density per unit area reduced and the galvanostatic discharging potential of Al anode plate shifted negative, discharge voltage was stability, and anodic polarization was small. When the current density was 200 mA/cm^2, the stable potential was about −1.735 V after annealing at 250 °C for 10 h; after annealing at 300 °C for 10 h, the stable potential was about −1.740 V; and after annealing at 350 °C for 10 h, the stable potential was about −1.742 V, that is, the galvanostatic discharging potential of Al anode plate shifted negative a little. The more annealing temperature raised and annealing time extended, the more stable potential shifted negative

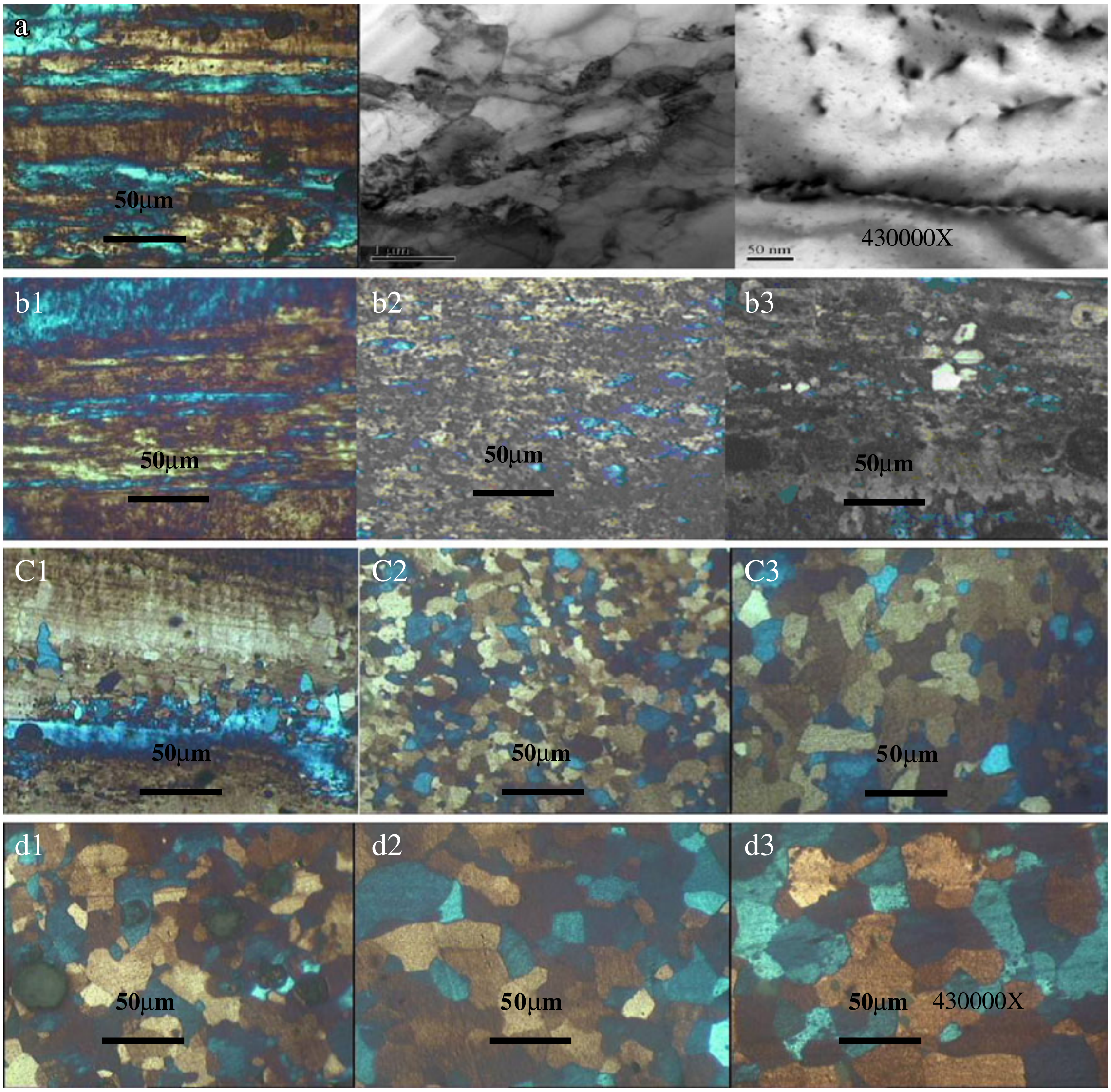

Fig. 5 Metallurgical micrographs of AM0501 Al alloy anode sheet after different annealing treatment. *a* Rolled. *b* 1–250 °C, 3 h; 2–250 °C, 6 h; 3–250 °C, 10 h. *C* 1–300 °C, 3 h; 2–300 °C, 6 h; 3–300 °C, 10 h. *d* 1–350 °C, 3 h; 2–350 °C, 6 h; 3–350 °C, 10 h

(Fig. 9a–c). At 80 °C in the 4 mol/l NaOH +10 g/l Na_2SnO_3 medium and when the current density is 800 mA/cm^2, the galvanostatic discharging time curve was shown in Fig. 9d. From the picture, we can see that AM0501 aluminum alloy anode still had a very high electrochemical activity even in high current density conditions. And stability electrode potential was still very negative. During the discharge process, the discharge curves were smooth and electrode

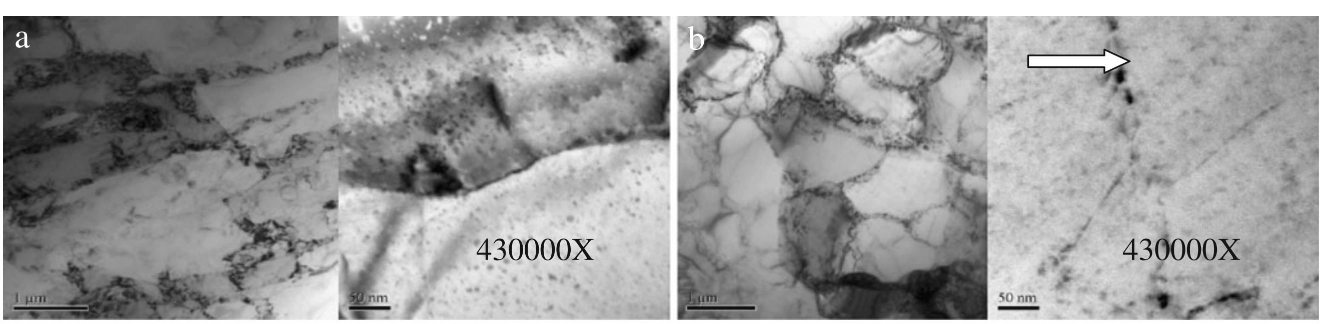

Fig. 6 TEM of annealed AM0501 Al alloy anode sheet. **a** 250 °C, 6 h; **b** 2–350 °C, 10 h

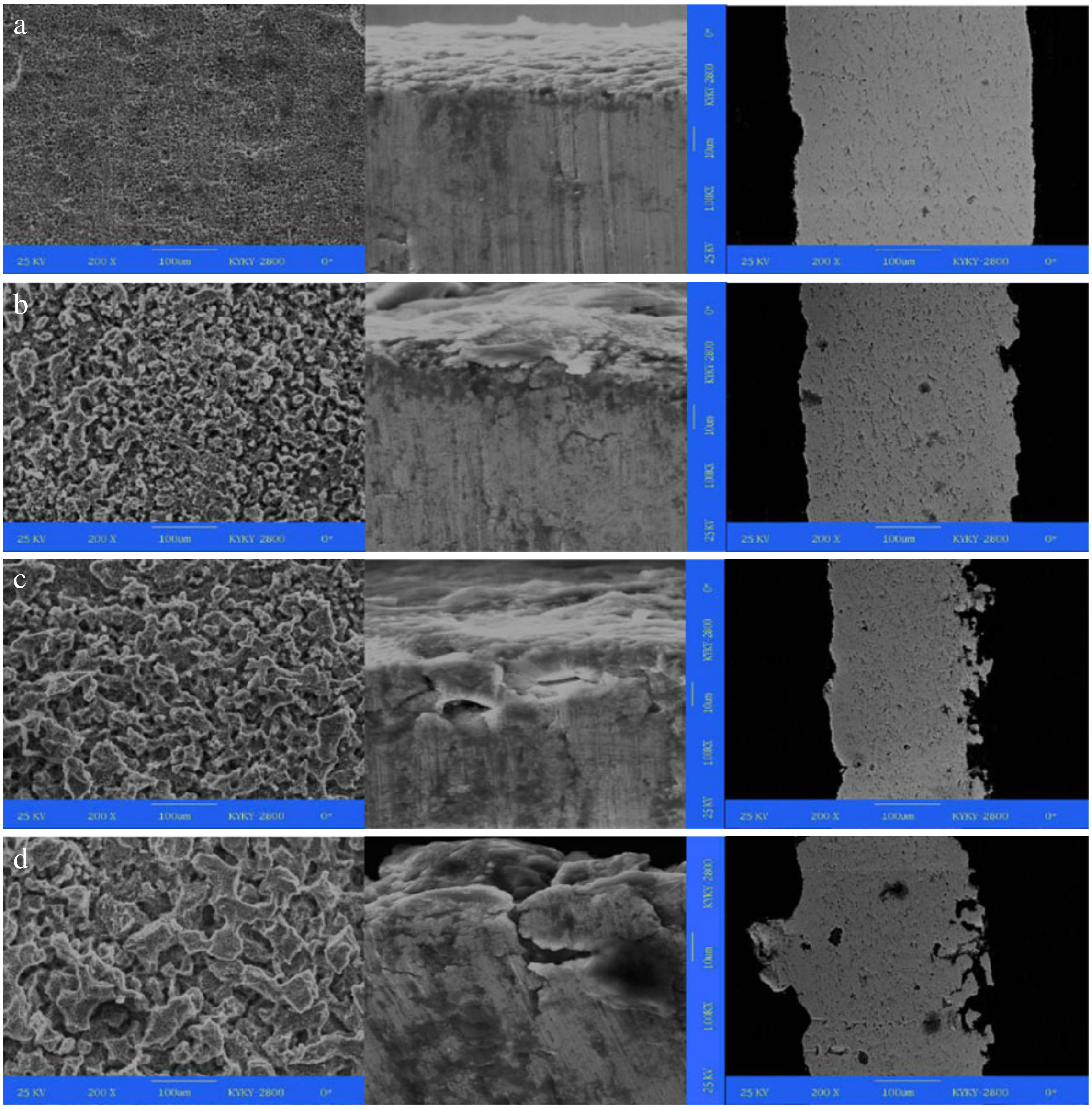

Fig. 7 Surface and section morphologies of AM0501 Al alloy anode sheet after corrosion. **a** Rolled; **b** 250 °C, 6 h; **c** 300 °C, 6 h; **d** 350 °C, 6 h

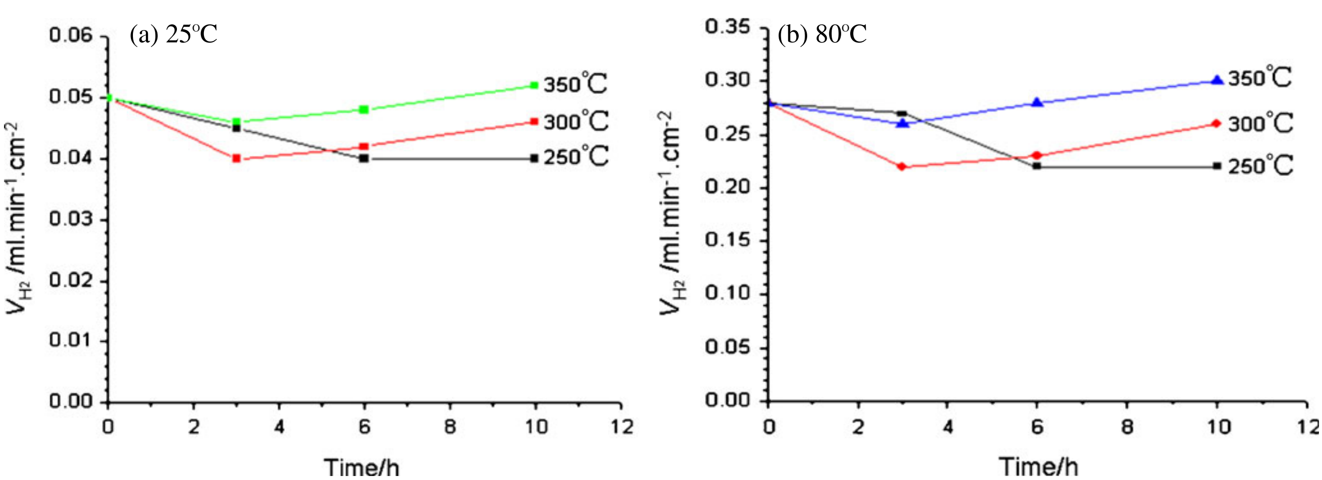

Fig. 8 Hydrogen evolution rate of AM0501 Al alloy anode sheet after annealing treatment (4 mol/l NaOH+10 g/l Na_2SnO_3)

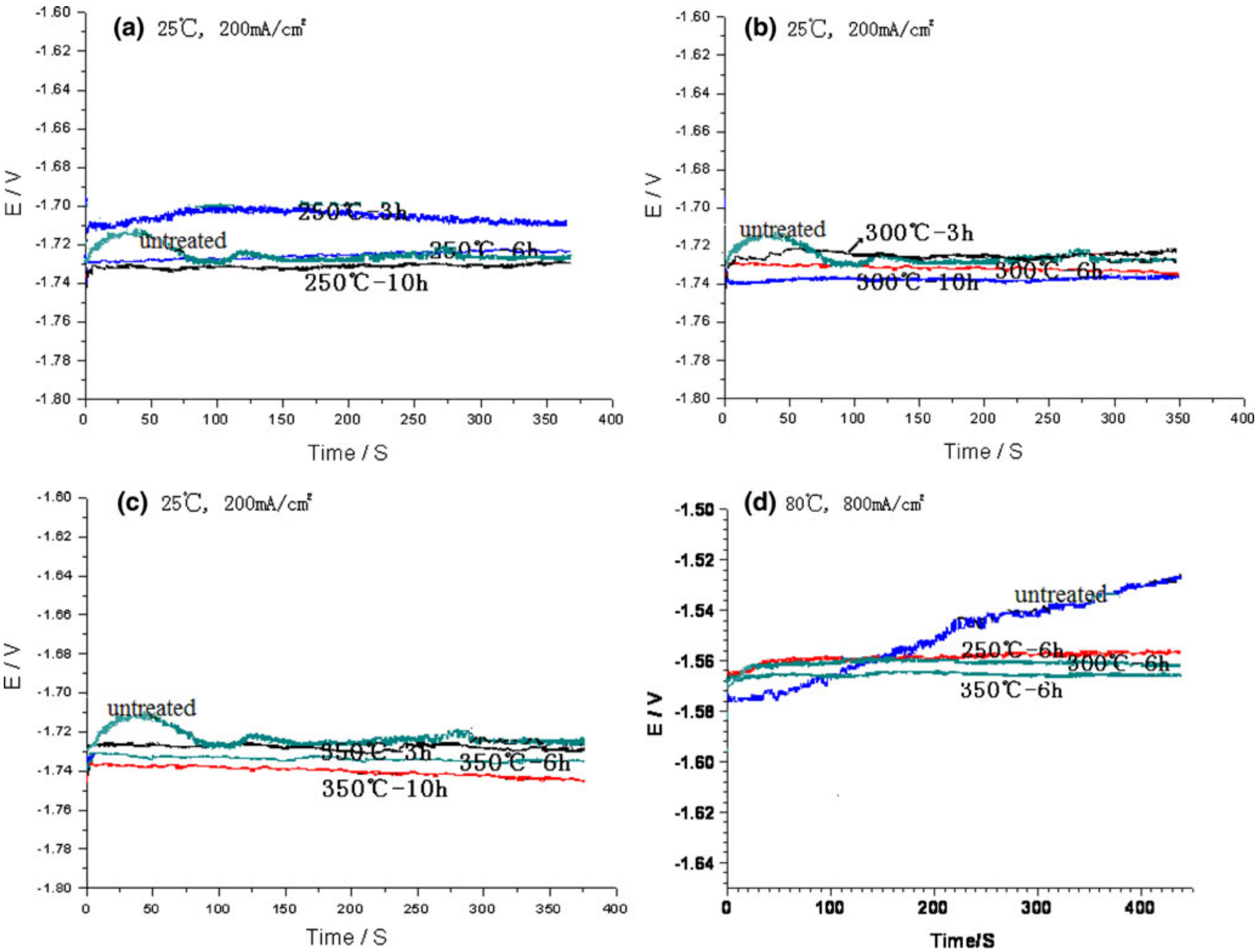

Fig. 9 Galvanostatic curves of AM0501 Al alloy anode sheet. Electrolyte—4 mol/l NaOH+10 g/l Na_2SnO_3

potential was stability. Besides, unannealed AM0501 aluminum alloy anode potential was extremely unstable, and the potential was more positive. After annealing at 250 °C for 6 h, at 300 °C for 6 h, and at 350 °C for 6 h, the stable potentials of AM0501 aluminum alloy anode materials were separately −1.560, −1.562, and −1.564 V. With the increase of annealing temperature, stable potential shifted negative.

Conclusions

1. When homogenization treated at 500 °C, 550 °C, and 600 °C, the microstructure and the corrosion rate (hydrogen evolution rate) of AM0501 alloy anode material did not change much. It means that the temperatures have little effect on improving the properties of this material. Besides, with the increase of temperature and time, the electrode potential shifted positive slightly.
2. The 0.45-mm-thick cold-rolled AM0501 aluminum alloy plate (cold deformation 94%) annealing at different temperatures and time (250 °C≤10 h, 300 °C≤3 h) will have some changes in microstructure. Its microstructure was similar with that of the cold-rolled state organizations, which is the “plate-shaped head” fibrous tissue in return annealing stage. After annealing at 250 °C for 10 h and at 300 °C for 3 h, the microstructure of fibrous tissue became recrystallization and some of the new grain replaced the old lath grains. It was the initial process of recrystallization. After annealing at 300 °C for 6 h, sub-grain boundaries completely disappeared, forming a lot of small polygonization grains. After annealing at 350 °C for 6 h and at 350 °C for 10 h, fine-grained microorganization was almost completely disappeared and became to coarse equiaxed recrystallization texture, forming a relatively uniform coarse grain. This was the grain growth process followed with recrystallization. At the same time, the

grain boundary precipitates accompanied by the ball phenomenon.

3. At the galvanostatic discharging process, the potential of AM0501 rolled aluminum alloy anode plate was extremely unstable, the hydrogen evolution rate was very large, and the corrosion was non-uniform. While after reply annealing treatment hydrogen evolution rate of AM0501 aluminum alloy anode plate decreased, potential was stable and stable potential shifted negative. After recrystallization annealing process, hydrogen evolution rate of AM0501 aluminum alloy anode plate increased with the increase of annealing temperature and time, and stable potential negative shift reduced.

Acknowledgment This work was supported by COSTIND of China (no. JPPT-115-2-747).

References

1. ZQ MA et al (2009) Trans Nonferrous Met Soc China 19:160–165
2. Luo QQ (2002) Aluminum melting and casting. Guangdong Science and Technology, Guangdong
3. Peng DS (2004) Aluminum melting and casting. Central South University Press, Changsha
4. Guy AG, Hren JJ (1981) Principles of physical metallurgy. Machinery Industry, Beijing
5. Cui ZhQ, Liu BX (1998) Principles of metallurgy and heat treatment. Harbin Institute of Technology, Harbin
6. Ge XL, Yang XH (2004) Metal materials and heat treatment. Shanghai Science and Technology, Shanghai
7. Zhang YY, Qi GT (2005) Metallic Funct Mater 12(2):25–30
8. Zhang LSh, Wang ShY, Wang W (2006) Power Source Technology 130:1000–1002
9. Qu JE, Qi GT, Zhang L (2002) Corrosion Sci Protect Tech 14 (3):169-172
10. Ma ZQ (2001) J Mater Sci Eng 24(6):89–95
11. Qi GT, Guo ZhH, Wei BK (2000) Transact Mat Heat Treat 21 (4):68–72
12. Wang DL, Lin L, Zhu RQ (1992) Materials Development Application 7(3):38-45
13. Crevecoeur C, Wit HJ (1987) Electrochem Soc 134(4):808–816
14. Qi HF, Liang GCh, Li GL (2005) Cell 35(4):306–307
15. Lin ShY, Tian Sh (2006) Hot Working Technol 35(18):50–52
16. Mao WM, Zhang XM (2005) Quantitative analysis of crystal texture. Metallurgical Industry Press, Beijing
17. Huang T, Qu JH, Wang F (2005) Light Alloy Fabrication Technol 4:37–40
18. Liu ChM, Zhang XM, Chen ZY (2001) Journal of Central South University of Technology, 1(1):85-88
19. Li DCh, Li WX (2006) Baotou Iron Steel Inst 1:43–46
20. Yang JJ (2006) Jianghan Univ 6(2):36–38
21. Yang GCh, Zhang HY, Long XH (2001) Met Heat Treat 1(1):21–23
22. Deng YL, Zhang XM, Liu Y (2006) Rare Met Mater Eng 2:195–198
23. Xiao YQ, Zhang XM, Jin L (2003) Mater Guide 6(6):80–83
24. Jin L, Zhang XM, Xiao YQ (2003) Chin J Nonferrous Met 2 (1):1–4
25. Mao WM, Yang H, Yu YN et al (2003) China Nonferrous Met 10:1057–1060
26. Liu Y, Zhang XM, Deng YL et al (2007) Phys examination Phys Test 43(7):346–348
27. Ma ZQ, ZUO L, Pang X, Zeng SM (2007) Transitions Nonferrous Met Soc China 19(1):160–165
28. Breslin CB, Carroll WM (1992) Corros Sci 33(11):1735
29. Marilyn J, Niksa J, Wheeler J (1988) Aluminum-oxygen batteries for space applications. J Power Sources 22:261–267
30. Krishnan M, Subramanyan N (1977) Corrosion Sci 17(10):893–900
31. Ddspic AR (1983) Electrochemical power conversion [A]. Proc of the 29th IUPAC Congress Cologne[C]. Federal Republic of Germany, June
32. Reboull MC, Gimenez PH, Rameau JJ (1984) A proposed activation mechanism for Al anodes. Corrosion 40:366
33. Dow EG, Bessette RR, Seeback GL, Orndorff C (1997) J Power Sources 65(30):207–212